

25 **Abstract**

26 Faster relearning of an external perturbation, savings, offers a behavioral linkage between motor
27 learning and memory. To explain savings effects in reaching adaptation experiments, recent
28 models suggested the existence of multiple learning components, each shows different learning
29 and forgetting properties that may change following initial learning. Nevertheless, the existence of
30 these components in rhythmic movements with other effectors, such as during locomotor
31 adaptation, has not yet been studied. Here, we study savings in locomotor adaptation in two
32 experiments; in the first, subjects adapted to speed perturbations during walking on a split-belt
33 treadmill, briefly adapted to a counter-perturbation and then readapted. In a second experiment,
34 subjects readapted after a prolonged period of washout of initial adaptation. In both experiments
35 we find clear evidence for increased learning rates (savings) during readaptation. We show that
36 the basic error-based multiple timescales linear state space model is not sufficient to explain
37 savings during locomotor adaptation. Instead, we show that locomotor adaptation leads to changes
38 in learning parameters, so that learning rates are faster during readaptation. Interestingly, we find
39 an inter-subject correlation between the slow learning component in initial adaptation and the fast
40 learning component in the readaptation phase, suggesting an underlying mechanism for savings.
41 Together, these findings suggest that savings in locomotion and in reaching may share common
42 computational and neuronal mechanisms; both are driven by the slow learning component and are
43 likely to depend on cortical plasticity.

44

45 **Introduction**

46 Our motor system is known for its ability to rapidly adapt to changes in the environment and
47 changes of its own (Scheidt et al. 2000; Thoroughman and Shadmehr 2000). It was suggested that
48 such adaptation depends on an error-based process which gradually updates one's controller based
49 on the discrepancy between forward model predictions and sensory inputs (e.g., sensory prediction
50 errors) (Shadmehr and Mussa-Ivaldi 1994). For example, when humans start to walk on split-belt
51 treadmill imposing different speeds to each leg, the sensory consequences of the motor commands
52 are different than expected, causing kinematic (Reisman et al. 2005) and kinetic (Mawase et al.
53 2013) motor errors. Exposed to such perturbation, subjects gradually modulate the walking speed
54 of each leg to adapt to the speed imposed by the treadmill. Interestingly, this learning process led
55 to the formation of a motor memory that can be recalled later (Malone et al. 2011; Shadmehr and
56 Brashers-Krug 1997).

57 Faster relearning of the same perturbation when introduced again (i.e. savings) receives great
58 attention in the motor control community since it reflects the formation of a new motor memory.
59 Initial attempts to model adaptation to an external perturbation were based on state space models
60 composed of a fast and one or multiple slow processes (Lee and Schweighofer 2009; Smith et al.
61 2006). However, these linear multiple-rate state space models could not explain savings that occur
62 after a prolonged period of washout (Krakauer et al. 2005; Zarahn et al. 2008), and across days
63 (Robinson et al. 2006). Instead, a recently non-linear state space model (Zarahn et al. 2008) and
64 context-dependent models (Ingram et al. 2011; Lee and Schweighofer 2009) were suggested to
65 better explain a variety of phenomena reported in the motor adaptation literature, including
66 savings. While evidence for savings has been accumulated from different systems [saccades, arm
67 reaching, and locomotion (Kojima et al. 2004; Krakauer et al. 2005; Malone et al. 2011)] and
68 across paradigms [saccades, visuomotor and force field adaptation (Kojima et al. 2004; Krakauer
69 et al. 2005; Smith et al. 2006; Zarahn et al. 2008)], adaptation and savings were mainly modeled
70 based on reaching and saccades adaptation results, and to the best of our knowledge, was never
71 modeled for locomotor adaptation. The generalization of adaptation models which were
72 constructed based on reaching experiments to locomotor adaptation is questionable, as the two
73 behaviors differ greatly in terms of neuronal substrates, the nature of the behavior, and the role of
74 visual feedback: locomotion is rhythmic, depends greatly on central pattern generators located in
75 the spinal cord and shows adaptation at the spinal cord level (Heng and de Leon 2007), whereas
76 reaching movements are discrete, guided by visual input and depend on cortical substrates.

77 Recently, savings in locomotor adaptation was reported in a set of psychophysical experiments
78 (Malone et al. 2011). In these studies savings across days was found even after a washout of initial
79 learning, suggesting that savings in locomotion reflect enhanced learning and not residual state
80 components. Nevertheless, locomotor adaptation was never formally modeled using state space
81 models, and the nature of parameter changes following initial adaptation has not been examined
82 yet.

83 Commonalities between the computational components leading to adaptation and savings of
84 reaching and locomotor adaptation may shed light on the neuronal and mechanistic basis of motor
85 savings.

86 Here we investigate the computational basis of locomotor adaptation by comparing the
87 performance of a linear dual-rate state space model with state space models with changing
88 parameters (Zarahn et al. 2008), under the hypothesis that locomotor adaptation leads to changes
89 in learning parameters that would last beyond the decay of the hidden state of the system.
90 Furthermore, we were interested in the relationship between the initial and second adaptation
91 phases, hypothesizing that the magnitude of savings will be correlated with the learning achieved
92 during the initial exposure to adaptation. Recent results suggest that long term retention (savings)
93 is affected by the slow learning process (Joiner and Smith 2008), and that the slow process may
94 be sensitive to reward whereas the fast process is not (Huang et al. 2011). Furthermore, Berniker
95 and Kording (2011) recently suggested that the fast and slow processes represent assignment of
96 the source of the error to internal and external perturbations, respectively. All these perspectives
97 suggest that savings may be the outcome of a slow learning and slow decaying process. By fitting
98 slow and fast learning components to the adaptation and readaptation phases independently we can
99 investigate the relationship between the above learning parameters.

100 The current study has two main aims. The first is to study the nature of savings in locomotor
101 adaptation by comparing linear and non-linear state space models. The second aim was to explore
102 the relationship of the slow and fast learning components before and after learning.

103

104 **Materials and Methods**

105 *Subjects.* Forty subjects (23 males, 17 females, mean age 25.9 ± 2.7 years) participated in the current
106 study. All subjects were naïve to our paradigm, without neurological history and without known
107 disturbances in walking. Subjects signed the informed consent form as stipulated by the
108 Institutional Helsinki Committee.

109

110 *Apparatus and general experimental procedure*

111 Subjects were instructed to walk on a custom split-belt force treadmill (ForceLink BV, Clemborg,
112 The Netherlands), which has two separate belts and an embedded force plate (Fig. 1A). The speed
113 and the direction (forward vs. backward) of each treadmill belt were controlled independently. The
114 belt's speed could be in one of two conditions, either moving together at same speed (tied-belts)
115 or moving separately at different speeds (split-belts).

116 Subjects were positioned in the middle of the split-belt treadmill with one foot on each belt. They
117 were instructed to look straight forward, preventing the usage of available visual feedback from
118 the environment regarding the speeds of the belts. For safety, all subjects wore a safety harness
119 that was suspended from the ceiling, two emergency stop buttons were available during the
120 experiment and two adjustable side bars were available to prevent falls. The safety harness and the

121 side bars did not support the subjects during the experiments. Custom software written in C#
122 (Microsoft Visual Studio, Washington State, USA) was used for controlling the speed of the belts
123 and the timing of the experiments.

124 Center of pressure (COP) data was sampled and recorded using Gaitfors[®] software (ForceLink
125 BV, Clemborg, The Netherlands). The system recorded the COP data at 500 Hz using 1-dimension
126 force sensors from a single large (160x800 mm) force plate embedded in the treadmill. COP is
127 defined as the projection of the resultant vertical force vector on the ground plane (Benda et al.
128 1994). Determining the two coordinates (x and y) of the COP is based on measuring the force
129 component from each force transducer placed on the corner of the force platform (Besser et al.
130 1993). The system was also able to determine representative gait events such as initial contact (IC)
131 and toe off (TO) for each leg independently (Roerdink et al. 2008). In this study, our primary
132 adaptation measurement was *COP symmetry* which has previously been shown as a robust
133 adaptation index (Mawase et al. 2013). *COP symmetry* was defined as follows:

$$134 \quad COP \text{ Symmetry} = \frac{\text{Left COP length} - \text{Right COP length}}{\text{Left COP length} + \text{Right COP length}} \quad (1)$$

135 where left COP length was calculated as the y (anterior-posterior) distance in the COP profile
136 between consecutive left TO and right IC and right COP length was calculated as the y distance
137 between consecutive right TO and left IC (Fig. 1B). The difference was then normalized to the
138 sum of the right and left COP length.

139 Our aim was to understand what drives adaptation and savings during locomotion. Predominantly,
140 we aimed to test the learning process that underlies locomotor adaptation. To answer this question,
141 we began with reanalyzing previously collected data from Mawase et al. (2013) (experiment 1).
142 We followed up with two additional experiments (experiments 2 and 3) in which we tested the
143 best variation of the linear state-space model (SSM) that explains savings during locomotor
144 adaptation.

145

146 *Experiment 1: Adaptation-Washout (AW) paradigm*

147 For experiment 1, we reanalyzed data of ten subjects (6 males, 4 females, mean age, 25.8±3.4
148 years) from a dataset previously reported by Mawase et al. (2013). For all subjects, the self-
149 identified dominant leg was the right leg. Leg dominance was determined by asking each subject
150 about the leg he/she uses to kick a ball. All subjects completed three blocks: *baseline*, *adaptation*
151 and *washout* (Fig. 1C left panel). During the *baseline* block, subjects walked with both belts at
152 same speed for 6 minutes. They started with the “slow” speed, then at “fast” speed, and finally at
153 “slow” speed for 2 minutes at each speed. We define “slow” and “fast” speeds to be 0.5 m/s and 1
154 m/s respectively. During *adaptation*, subjects walked with the belts of the split-belt treadmill
155 moving at different speeds for each leg for 15 minutes. The belt of the left (non-dominant) leg

156 moved always at the slow speed while the belt of the right leg moved at the fast speed. During
157 *washout*, the belts were set again to move together at the slow speed (0.5 m/s) for 5 minutes.

158 The aim of reanalyzing the AW experiment was to test whether the traditional single/dual rate
159 SSM (Smith et al. 2006), designed to study reaching adaptation, could also account for locomotor
160 adaptation. In particular, the purpose was to test whether the models can capture the shape of the
161 error reduction and the after effect curves seen following removal of the perturbation (i.e.
162 washout).

163

164 *Experiment 2: Adaptation-Counterperturbation-Readaptation paradigm*

165 Seventeen naïve subjects (10 males, 7 females, mean age 26.1 ± 1.8 years) participated in
166 experiment 2. For sixteen subjects, the self-identified dominant leg was the right leg. Subjects in
167 the counterperturbation experiment completed four walking blocks: *baseline*, *adaptation*,
168 *adaptation to counterperturbation* and *readaptation* (Fig. 1C middle panel). All subjects
169 experienced 2 minutes of baseline walking on tied-belts. They walked one minute at “slow” speed
170 (0.6 m/s) followed by another one minute at “fast” speed (1.2 m/s). All subjects were then adapted
171 to split-belts (belts split at 0.6 and 1.2 m/s; slow belt under dominant leg) for 10 minutes. Subjects
172 were then briefly adapted with opposite split-belts (belts split at 1.2 and 0.6 m/s; fast belt under
173 dominant leg) for 30 seconds. All subjects were then readapted to the split-belts presented at the
174 first adaptation block, again for 10 minutes, (belts split at 0.6 and 1.2 m/s; slow belt under dominant
175 leg).

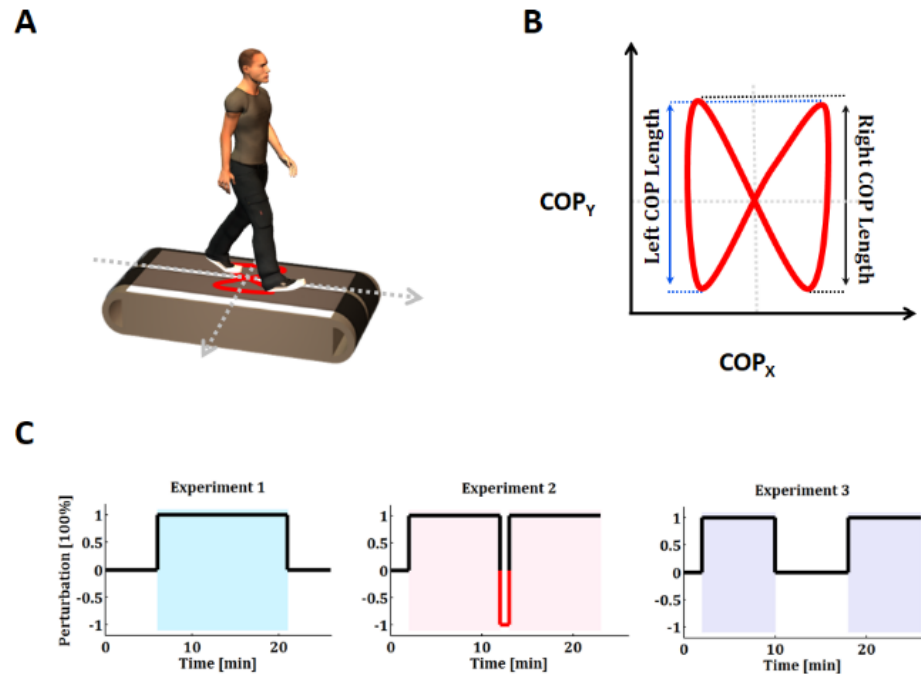
176

177 *Experiment 3: Adaptation-Washout-Readaptation paradigm*

178 Thirteen naïve subjects (7 males, 6 females, mean age 25.7 ± 1.9 years) with right dominant leg
179 participated in experiment 3. Subjects in the washout experiment completed four walking blocks:
180 *baseline*, *adaptation*, *washout* and *readaptation* (Fig. 1C right panel). All subjects experienced 2
181 minutes of baseline walking on tied-belts. Then they walked one minute at “slow” speed (0.6 m/s)
182 followed by another one minute at “fast” speed (1.2 m/s). All subjects were then adapted to split-
183 belts (belts split at 0.6 and 1.2 m/s; slow belt under dominant leg) for 8 minutes. Subjects were
184 then washed out with the slow tied-speed (belts tied at 0.6 m/s) for 8 minutes. All subjects were
185 then readapted to the same split-belts presented in the first adaptation block (belts split at 0.6 and
186 1.2 m/s; slow belt under dominant leg) for 8 minutes.

187

188 **Figure 1.** Experimental
 189 design and protocols. **A.**
 190 Subjects walked on a
 191 split-belt force
 192 treadmill with two
 193 separated belts and an
 194 embedded force plate
 195 (white plate). Red trace
 196 represents the COP
 197 profile for one gait
 198 cycle. **B.** Schematic
 199 example for one COP
 200 profile for one cycle.
 201 Left COP length was
 202 calculated as the y
 203 (anterior-posterior)
 204 distance in the COP
 205 profile between



206 consecutive left TO and right IC and right COP length was calculated as the y distance between
 207 consecutive right TO and left IC. **C.** Left panel - protocol of experiment 1: baseline (6 min), adaptation
 208 (15 min) and washout (5 min). During the baseline block, subjects walked with both belts at same
 209 speed (tied-belts) [0.5:0.5 m/s (2 min), 1:1 m/s (2 min) and 0.5:0.5 m/s (2 min)]. During adaptation,
 210 subjects walked with different speeds (split-belts) (0.5:1 m/s). During washout, subjects walked on
 211 tied-belts at slow speed condition (0.5:0.5 m/s). Middle panel - protocol of experiment 2: baseline (2
 212 min), adaptation (10 min), counterperturbation (30 sec) and readaptation (10 min). During the
 213 baseline block, subjects walked on tied-belts [0.6:0.6 m/s (1 min), 1.2:1.2 m/s (1 min)]. During
 214 adaptation, subjects walked on split-belts (0.6:1.2 m/s; slow belt under dominant leg). During
 215 counterperturbation, the belts were set to the opposite split-belts pattern (1.2:0.6 m/s). All subjects
 216 were then re-exposed to the same split-belts, as in the adaptation block, again for 10 min, (0.6:1.2
 217 m/s; slow belt under dominant leg). Right panel - protocol of experiment 3: baseline (2 min),
 218 adaptation (8 min), washout (8 min) and readaptation (8 min). Speed condition in each block of
 219 experiment 3 was similar to experiment 2.

220

221 *Modeling*

222 Different variations of the SSM have been recently suggested to explain adaptation and savings
 223 during force field (Donchin et al. 2003; Smith et al. 2006), object rotation (Ingram et al. 2011) and
 224 visuomotor (Lee and Schweighofer 2009; Zarahn et al. 2008) perturbations. Most of these models
 225 assume linear time invariant (LTI) properties of the parameters (Donchin et al. 2003; Ingram et al.
 226 2011; Lee and Schweighofer 2009; Smith et al. 2006) while the rest model assumes varying
 227 parameters that change with experience (Berniker and Kording 2011; Zarahn et al. 2008). All of
 228 these error-based models suggest that trial-by-trial adaptation occurs by updating the appropriate

229 internal models (i.e. states) to reflect the behavior of the perturbation. However, the varying
 230 parameter model suggests that motor adaptation occurs by updating the parameters along with the
 231 states. In the current study, we compare the prediction of three variations of the proposed SSM
 232 during locomotor adaptation: (1) dual-rate linear time invariant SSM (Smith et al. 2006), (2)
 233 single-rate varying parameters SSM (Zarahn et al. 2008), (3) dual-rate varying parameters SSM
 234 (Zarahn et al. 2008). The equations of the models took the following forms:

235 (a) Dual-rate SSM:

$$e(n) = D \cdot f(n) - y(n)$$

$$y(n) = x_f(n) + x_s(n)$$

236 $x_f(n+1) = A_f \cdot x_f(n) + B_f \cdot e(n)$

$$x_s(n+1) = A_s \cdot x_s(n) + B_s \cdot e(n)$$

$$A_f < A_s < 1, B_s < B_f < 1$$

237

238 (b) Single-rate varying parameters SSM

$$e(n) = D \cdot f(n) - y(n)$$

239 $y(n) = x(n)$

$$x(n+1) = A(p) \cdot x(n) + B(p) \cdot e(n)$$

240

241 (c) Dual-rate varying parameters SSM

$$e(n) = D \cdot f(n) - y(n)$$

$$y(n) = x_f(n) + x_s(n)$$

242 $x_f(n+1) = A_f(p) \cdot x_f(n) + B_f(p) \cdot e(n)$

$$x_s(n+1) = A_s(p) \cdot x_s(n) + B_s(p) \cdot e(n)$$

$$A_f(p) < A_s(p) < 1, B_s(p) < B_f(p) < 1$$

243 In a given trial n , $e(n)$ is the motor error, $f(n)$ is the external perturbation (defined as the
 244 difference between left and right belt speeds) and $y(n)$ is the net motor output on the same trial
 245 (i.e. the state of the learner). $A(p)$ and $B(p)$ are the forgetting and learning rate constants that
 246 change with an experience p , respectively. Experiments 2 and 3 contain three experience phases:
 247 adaptation-counterperturbation-readaptation in experiment 2 and adaptation-washout-readaptation
 248 in experiment 3. D is a compliance scalar with units of seconds per meter. The *dual-rate SSM*
 249 suggests that the net motor output has two inner states $x_f(n)$ and $x_s(n)$, where $x_f(n)$ is the fast
 250 process that reacts rapidly to motor error but has weak memory retention and $x_s(n)$ is the slow
 251 process that reacts slowly to motor error but significantly exhibits strong retention. To this end, it
 252 contains five free constant parameters (A_f, B_f, A_s, B_s, D). In the *single-rate varying parameters*
 253 *SSM*, there is only single learning process $x(n)$, which has varying forgetting and learning
 254 parameters $A(p)$ and $B(p)$, respectively. This model contains seven free parameters [

255 $A_{adaptation}, B_{adaptation}, A_{Deadaptation}, B_{Deadaptation}, A_{Readaptation}, B_{Readaptation}, D$] and [
 256 $A_{adaptation}, B_{adaptation}, A_{Washout}, B_{Washout}, A_{Readaptation}, B_{Readaptation}, D$] for experiment 2 and 3, respectively.
 257 Finally, the *dual-rate varying parameters SSM*, which has 13 free parameters, suggests that the net
 258 motor output has a single state in the fast process and a single state in the slow process for each
 259 experience phase (i.e. adaptation/ counterperturbation/ washout/ readaptation). In addition, the
 260 motor output/perturbation [i.e. $y(n)/f(n) = 1 - e(n)/f(n)$] represents the predicted amount of
 261 adaptation in each trial.

262 We searched for the best model that simultaneously accounts for adaptation and savings during
 263 locomotion. Model selection was performed by the Akaike Information Criterion (AIC) (Akaike
 264 1974), computed for the single subject data. For each candidate model, the AIC value reflects the
 265 combination of fitting amount along with the number of free parameters, and the optimal model is
 266 identified by the minimum value of AIC. Thus, the difference in AIC values of two candidate
 267 models would provide strong indication toward the best fitting model.

$$268 \quad AIC = 2 \cdot k - n \cdot \ln(L) \quad (2)$$

269 where k is the number of free parameters, n is the number of data points and L is the maximized
 270 value of the likelihood function for the estimated model. Under the assumption that the model
 271 errors are independent and identically normally distributed (i.i.d), we can rewrite the criterion as
 272 follow:

$$273 \quad AIC = 2 \cdot k + n \cdot \ln(\sigma_r^2) \quad (3)$$

274 where σ_r is the standard deviation of the residual errors between the actual and predicted data.
 275 AIC analysis is critical for our study to account for the increase in number of free parameters
 276 introduced in the varying parameters SSM models.

277 We estimated the parameters of the models by using the *fmincon* routine performed by Matlab that
 278 maximized the log likelihood. In all experiments, the estimated error of each model was fitted to
 279 the individual subject's data. In experiment 2 and 3, the estimated error was fitted simultaneously
 280 to all three phases. Thereafter, we calculated the mean and the standard error for each parameter
 281 in each experiment phase for further comparison analysis.

282 For each adaptation and readaptation phase and for each individual subject, we quantified the
 283 initial error as the motor error of the first trial and mid-error as the average of the trials 2-30. This
 284 method has previously been shown as a robust savings measurement index (Malone et al. 2011).
 285 Following the definition of savings by previous works as an increase in the rate of error reduction
 286 following initial learning (Huang et al. 2011; Malone et al. 2011; Zarahn et al. 2008), we fit a
 287 single exponential function, which has the form $y(n) = a \cdot e^{-n/b} + c$, to each subject's data to
 288 estimate the rate of error reduction. Moreover, savings was also quantified as the difference

289 between mid-errors across the two adaptation blocks. In addition, we defined “initial bias” as the
290 difference between initial errors across the two adaptation blocks.

291 *Statistical Analysis.* Statistical analysis of the data was performed using the Matlab software with
292 Statistics Toolbox (The MathWorks Inc., Natick, MA, USA). We used repeated measure analyses
293 of variance (ANOVA_{RM}) to compare differences between AIC values of the models in experiment
294 2 and 3. When significant differences were found, post hoc analyses were performed. The Shapiro-
295 Wilk W test with alpha level of 0.05 was used to assess the t-test assumption of normality on the
296 AIC difference values across subjects. When the p-value was greater than the chosen alpha level,
297 paired t-test was used to compare the difference in AIC between models. Otherwise, non-
298 parametric Wilcoxon matched-pair signed-rank test was used for comparison. Correlation between
299 learning parameters (i.e. B_f and B_s) and motor errors were evaluated using the Pearson correlation
300 coefficients. The free parameters and their confidence intervals of the single exponential function
301 were estimated using the Matlab software with Curve Fitting Toolbox. Two-tailed t-test was used
302 to compare initial error and mid error in experiment 2 and 3. Significance level was set to 0.05.

303

304 **Results**

305 *Experiment 1- Learning processes in locomotor adaptation*

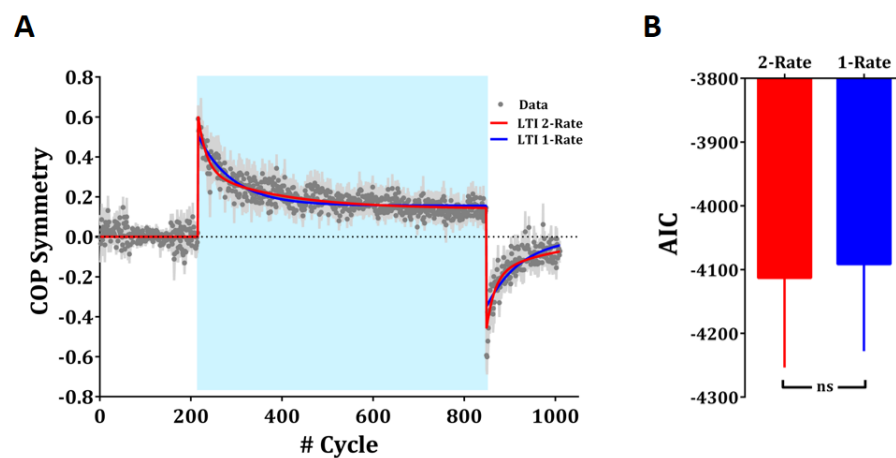
306 We first sought to test the hypothesis whether basic LTI single-rate or dual-rate learning process
307 could explain the fundamental principles of locomotor adaptation time course, i.e. the error
308 reduction during the perturbation block and, predominantly, the after effect during the washout
309 block. To this end, we reanalyzed our previous published data (Mawase et al. 2013). Fig. 2A shows
310 the learning process during adaptation to speed perturbation using the split-belt system. During the
311 baseline phase (i.e. zero perturbation), COP symmetry (i.e. motor error) values were close to zero,
312 mean error at the baseline phase across subjects was 0.007 ± 0.042 (mean \pm SD), which indicates
313 a symmetric pattern of locomotion. During early adaptation, there was a significant positive value
314 of the error. The mean error over the first two trials was 0.56 ± 0.077 (mean \pm SD). This positive
315 value of error decreased slowly throughout the adaptation phase, reaching an error rate of $0.128 \pm$
316 0.046 over the last 10 trials. In the early post-adaptation phase (washout), there was a clear negative
317 after-effect, indicated by mean error of -0.57 ± 0.079 over the first two trials. This reverse pattern
318 gradually returned to baseline values, reaching error value of -0.067 ± 0.047 over the last 10 trials.

319 We fit the single-rate SSM as well as the dual-rate SSM to the trial series of the motor error for
320 each subject from experiment 1. The single-rate model has one state, whereas the dual-rate model
321 proposed that the motor output has two independent states, a fast state that reacts rapidly to motor
322 error but has strong forgetting rate, and one slow state that reacts slowly to motor error but
323 significantly exhibits strong retention (See Materials and Methods). Since there is only one
324 adaptation phase in experiment 1, the single-rate LTI model is identical to the single-rate varying

325 parameters model. The two SSMs models were computed separately for each subject and
326 simultaneously to all phases of the experiment. The across-subject averages of the parameter
327 estimates from the single-rate SSM were $A=0.9939\pm 0.0017$ (mean \pm SEM), $B=0.0153\pm 0.0047$ and
328 $D=1.0944\pm 0.1429$, and the across-subject averages of the parameter estimates from the dual-rate
329 SSM were $A_{fast}=0.6885\pm 0.1367$ (mean \pm SEM), $A_{slow}=0.9979\pm 0.0009$, $B_{fast}=0.01781\pm 0.0827$,
330 $B_{slow}=0.0094\pm 0.0023$ and $D=1.3958\pm 0.1115$. To qualitatively illustrate the time courses of the
331 different SSMs during experiment 1, we fitted the two models to the across-subject averaged data
332 (Fig. 2A). As shown in Fig. 2A, the two models did a responsible job of explaining adaptation and
333 after-effect during the first experiment.

334

335 **Figure 2.** Group data and
336 model prediction during
337 experiment 1. **A.** Across-
338 subject averaged COP
339 symmetry (gray points)
340 in each gait cycle and the
341 fitted LTI single-rate SSM
342 (blue line) and dual-rate
343 SSM (red line). **B.** Across-
344 subject averaged Akaike
345 Information Criterion
346 (AIC) for the single-rate
347 SSM (blue bar) and for the dual-rate SSM (red bar), respectively. Error bars indicate SEM.



348

349 To select the best model, we used the Akaike Information Criterion (AIC) to account for the
350 different number of parameters in each model. For each candidate model, the AIC value reflects
351 the combination of the goodness of fitting along with the number of free parameters. That is, the
352 AIC difference between two candidate models would provide strong evidence in favor of the
353 model with the lower AIC value. To assess the normality assumption of the t-test on the AIC
354 difference values across subjects, we used the Shapiro-Wilk W test. We found that the W value
355 was insignificant at alpha level of 0.05, suggesting that the assumption of normality of the AIC
356 distribution is valid ($W=0.92$, $p>0.39$). Figure 2B shows the mean AIC across subjects for each
357 model. The AIC of the dual-Rate SSM (-4112.9 ± 140.6 , mean \pm SEM) was comparable to the AIC
358 of the single-rate model (-4091.4 ± 136.5 , mean \pm SEM). The t statistic reveals that no difference
359 was observed in the AIC of the two models (two-tailed paired t-test, $t(9)=1.83$, $p=0.11$), indicating
360 that both models fit well the behavioral data of the first experiment. However, neither savings nor
361 anterograde interference can be examined in this type of experimental paradigm. Therefore, we
362 designed two additional experiments to test these phenomena.

363 *Experiment 2- Savings in counterperturbation paradigm*

364 In the second experiment, we sought to quantify within-day savings effects, and to find whether
365 the single-rate or the dual-rate SSM, which showed a good fit to single phase locomotor adaptation,
366 can also explain the faster relearning phenomenon (e.g., savings). To this end, we asked subjects
367 to relearn the same split-belt perturbation after a brief counterperturbation period that erased the
368 initial adaptation (Fig. 3A). During counterperturbation phase, the error of the last 5 strides was
369 on average -0.64 ± 0.04 (mean \pm SEM), which is not significantly different ($t(16)=0.986$, $p=0.3385$)
370 from the magnitude of the -0.6 counter perturbation (defined as the difference between left (0.6
371 m/sec) and right (1.2 m/sec) belt speeds). This result indicates that subjects had completely erased
372 their initial adaptation but did not start adapting to the counterperturbation. Subjects exhibited
373 strong savings during relearning of the same perturbation. Mid-error during readaptation,
374 computed based on strides 2-30 (0.22 ± 0.04 , mean \pm SEM), was significantly lower (two-tailed
375 paired t-test, $t(16)=8.96$, $p<0.0001$) than the mid-error during adaptation (0.47 ± 0.03). That is,
376 following initial adaptation, subjects learned the perturbation significantly faster (Fig. 3B),
377 indicating the existence of savings. Furthermore, we measured the effect of savings by estimating
378 directly the learning rates during adaptation and readaptation before and after adaptation. Indeed,
379 the learning rate of the exponential function in the readaptation block (0.28 ± 0.1 trial⁻¹) was higher
380 ($t(16)=2.24$, $p<0.05$) than the learning rate of the initial adaptation block (0.04 ± 0.008 trial⁻¹) (Fig.
381 3C). We could not find evidence for initial bias; analyzing the error of the first trial revealed that
382 there was no deference in COP symmetry between adaptation and readaptation ($t(16)=1.66$,
383 $p=0.12$) (Fig. 3D).

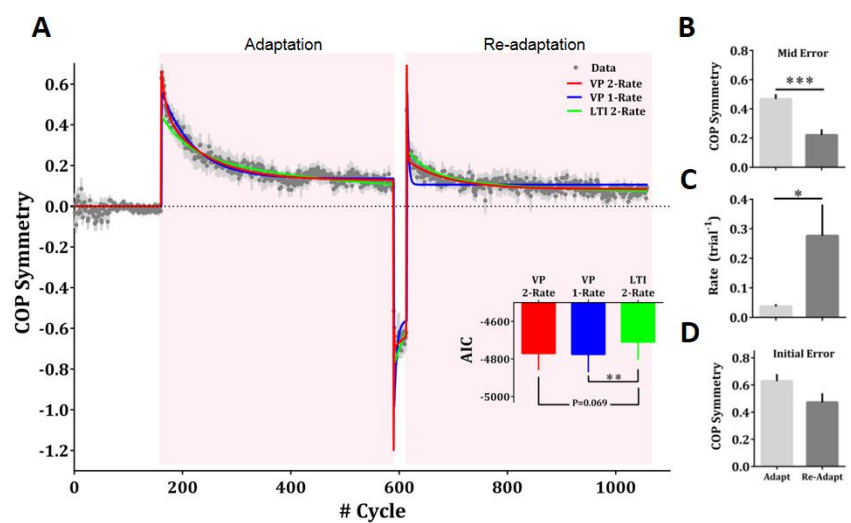
384 Three alternative models of the behavioral data in experiment 2 were compared. The first was the
385 LTI multiple timescales (i.e. LTI 2-Rate), which has two states, one fast and one slow (See
386 Materials and Methods). The second was the single-rate varying parameters SSM (i.e. VP 1-Rate),
387 which has a single learning process that has forgetting and learning parameters that could vary
388 across phases. The last one was the dual-rate varying parameters SSM (i.e. VP 2-Rate), which has
389 single state in the fast process and single state in the slow process with varying forgetting and
390 learning parameters. The varying parameter models were fitted for each phase separately, namely:
391 one fit for adaptation, one for counterperturbation and one for the readaptation phase. The three
392 SSMs models were computed separately for each subject and simultaneously to all three phases of
393 the experiment. The across-subject averages of the parameter estimates are provided in Table 1.
394 To qualitatively illustrate the time courses of the different SSMs during experiment 2, we fitted
395 the three models to the across-subject averaged data (Fig. 3A). As shown in Fig. 3A, the LTI 2-
396 Rate SSM did a responsible job of explaining adaptation and savings during readaptation.
397 Although the VP 1-Rate SSM did a good job explaining adaptation, it explained poorly savings
398 during readaptation, yielding too rapid readaptation. VP 2-Rate SSM fit well the averaged data
399 overall.

400 To select the best model, we again used the Akaike Information Criterion (AIC) to account for the
401 different number of parameters in each model. The Shapiro-Wilk W test on the AIC differences

402 across subjects reveals that none of the W values was significant, suggesting weak evidence to
 403 reject the null hypothesis of normally distributed population ($p > 0.47$). Inset shows the mean AIC
 404 across subjects for each model. ANOVA showed main effect of model on AIC measures
 405 ($F_{2,16} = 4.87$, $p < 0.05$). The AIC of the VP 1-Rate SSM (-4776.2 ± 23.0 , mean \pm SEM) was
 406 significantly lower (two-tailed paired t-test, $t(16) = 3.46$, $p < 0.01$) than that of the LTI 2-Rate SSM
 407 (-4710.0 ± 30.9). The AIC of the VP 2-Rate SSM (-4770.9 ± 21.6) tended toward being favored
 408 (two-tailed paired t-test, $t(16) = 1.95$, $p = 0.069$) over the LTI 2-Rate SSM.

409 To summarize experiment 2, the models with changing parameters between adaptation and
 410 readaptation explain the performance of single subjects better than the canonical two-rate state
 411 space model.

412 **Figure 3.** Group data and models predictions during
 413 experiment 2. **A.** Across-
 414 subject averaged COP
 415 symmetry (gray points).
 416 Colored lines represent the
 417 fits of the SSM models: green
 418 line represents the
 419 prediction of the LTI dual-
 420 rate SSM, blue line represents
 421 the prediction of the varying
 422 parameters single-rate SSM
 423 and red line represents the
 424 prediction of the varying
 425 parameters dual-rate SSM. Inset shows the across-subject averaged Akaike Information Criterion
 426 (AIC) for each model, respectively. **B.** Mid errors averaged across subjects during adaptation (light
 427 gray bar) and readaptation (dark gray bar). **C.** Average learning rate of a single exponential fit to
 428 individual subject data from adaptation (light gray bar) and readaptation (dark gray bar). **D.** Initial
 429 errors averaged across subjects during adaptation (light gray bar) and readaptation (dark gray bar).
 430 Error bars indicate SEM.



432

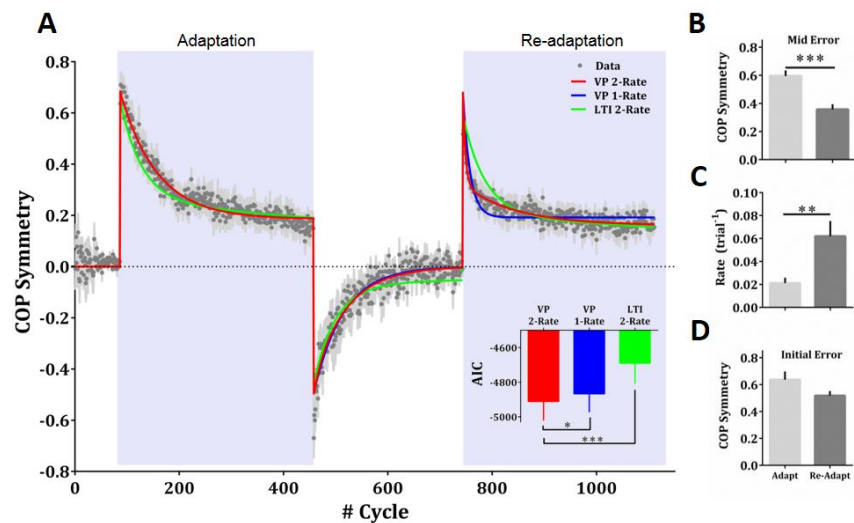
433 *Experiment 3- Savings in washout paradigm*

434 In the third experiment, we examined whether completely erasing the learned pattern by exposing
 435 subjects to a prolonged washout period would affect future locomotor savings, and whether one of
 436 the candidate SSM models could account for that. To this end, we asked subjects to relearn after a
 437 prolonged washout period (Fig. 4A). Comparing the mean errors of the last 5 strides of the washout
 438 phase (0.011 ± 0.03 , mean \pm SEM) and the mean errors of the last 5 strides of the baseline phase
 439 (0.014 ± 0.01 , mean \pm SEM) showed no significant differences in error rates (two-tailed paired t-
 440 test, $t(12) = 0.08$, $p > 0.9$), indicating that subjects had completely returned to their baseline

441 performance. Subjects demonstrated strong savings when they were re-exposed to the same
 442 perturbation for the second time. The mid-error during readaptation (0.36 ± 0.04 , mean \pm SEM)
 443 was significantly lower (two-tailed paired t-test, $t(12)=9.04$, $p<0.0001$) than the mid-error during
 444 adaptation (0.59 ± 0.04 , mean \pm SEM). Therefore, savings (i.e. the difference between the mid-
 445 errors) is significantly evident in the Adaptation-Washout-Readaptation experiment (One sample
 446 t-test, $t(12)=9.04$, $P<0.001$)(Fig. 4B). Estimating the learning rate of a single exponent function
 447 revealed similar results. We found that the estimated learning rate of the exponential function in
 448 the readaptation phase (0.06 ± 0.01 trial⁻¹) was higher ($t(12)=3.5$, $p<0.01$) than the time learning
 449 rate of the initial adaptation (0.04 ± 0.004 trial⁻¹) (Fig. 4C). Consistently with experiment 2,
 450 analyzing the error of the first trial revealed that there was no difference in COP symmetry between
 451 adaptation and readaptation ($t(12)=1.94$, $p=0.08$) (Fig. 4D).

452 Similarly to experiment 2, the three suggested SSMs models were computed separately for each
 453 subject and simultaneously in all three phases of the experiment. The across-subject averages of
 454 the parameter estimates are also provided in Table 1. To qualitatively illustrate the time courses of
 455 the different SSMs during experiment 3, we fitted the three models to the across-subject averaged
 456 data (Fig. 4A). As shown in Fig. 4A, the LTI 2-Rate SSM and the VP 1-Rate SSM could not
 457 capture the savings phenomenon during readaptation, whereas the VP 2-Rate SSM fit the averaged
 458 data very well overall.

459 **Figure 4.** Group data and models predictions during
 460 experiment 3. **A.** Across-
 461 subject averaged COP
 462 symmetry (gray points).
 463 Color lines represent the fits
 464 of the SSM models: green line
 465 represents the prediction of
 466 the LTI dual-rate SSM, blue
 467 line represents the
 468 prediction of the varying
 469 parameters single-rate SSM
 470 and red line represents the
 471 prediction of the varying
 472 parameters dual-rate SSM. Inset shows the across-subject averaged Akaike Information Criterion
 473 (AIC) for each model, respectively. **B.** Mid errors averaged across subjects during adaptation (light
 474 gray bar) and readaptation (dark gray bar). **C.** Average learning rate of a single exponential fit to
 475 individual subject data from adaptation (light gray bar) and readaptation (dark gray bar). **D.** Initial
 476 errors averaged across subjects during adaptation (light gray bar) and readaptation (dark gray bar).
 477 Error bars indicate SEM.



479 The inset in Fig. 4A shows the mean AIC across subjects for each model. To assess data normality,
 480 we used the Shapiro-Wilk W test on the AIC differences across subjects. We found two out of

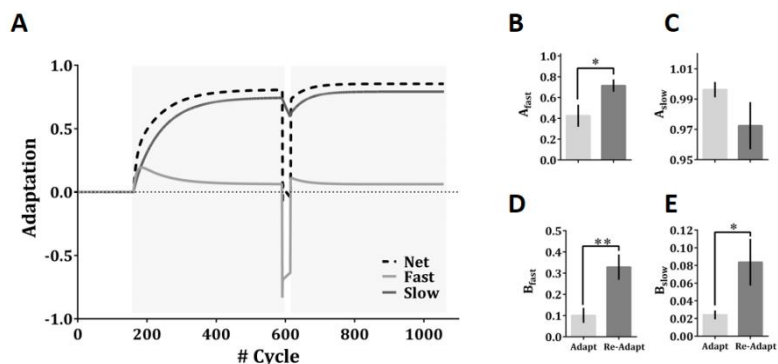
481 three W values were insignificant ($p > 0.08$), indicating that these differences are probably normally
 482 distributed. However, the W value of the AIC differences between VP 2-Rate and VP 1-Rate was
 483 significant ($P = 0.02$). To this end, we follow with non-parametric Wilcoxon matched pair signed-
 484 rank test to compare the difference between VP 2-Rate with VP 1-Rate. ANOVA showed main
 485 effect of model on AIC measures ($F_{2,12} = 15.64$, $p < 0.01$). We found the AIC of the VP 2-Rate SSM
 486 (-4911.5 ± 30.7 , mean \pm SEM) was significantly lower (two-tailed paired t-test, $t(12) = 4.692$,
 487 $p < 0.001$) than that of the LTI 2-Rate SSM (-4690.0 ± 32.9). Additionally, the AIC of the VP 2-
 488 Rate SSM was significantly lower (Wilcoxon matched pair signed-rank test, $p = 0.01$) than that of
 489 the VP 1-Rate SSM (-4867.3 ± 29.6).

490 To summarize experiment 3, the dual rate model with changing parameters between adaptation
 491 and readaptation after a prolonged period of washout explains the performance of single subjects
 492 significantly better than the canonical LTI dual rate model and the varying parameters single rate
 493 model.

494 *Parameter changes associated with savings*

495 Following the initial stages of model selection, showing that VP 2-Rate SSM explains savings
 496 effects better in experiment 3, we asked which parameters change following initial learning in both
 497 experiments. Figure 5A shows the slow and fast state estimates from the VP 2-Rate SSM to the
 498 across-subject averaged data during experiment 2. Both learning rates (i.e. B_f and B_s) and
 499 forgetting rates (i.e. A_f and A_s) changed following adaptation. Analyzing the across-subject
 500 averages of the parameter estimates reveals that the forgetting rate of the fast state (i.e. A_f) in
 501 adaptation (0.43 ± 0.1 , mean \pm SEM) was significantly lower (two-tailed t-test, $t(32) = 2.384$
 502 $p < 0.05$) than the forgetting rate of the fast state in readaptation (0.71 ± 0.06) (Fig. 5B), whereas the
 503 change of the forgetting rate of the slow state (i.e. A_s) was not significant (two-tailed t-test,
 504 $t(32) = 1.526$ $p = 0.14$) across blocks (0.99 ± 0.01 and 0.97 ± 0.02 in adaptation and readaptation,
 505 respectively) (Fig. 5C). Moreover, the learning rate of the fast state (i.e. B_f) in adaptation ($0.1 \pm$
 506 0.04) was significantly increased (two-tailed t-test, $t(32) = 3.291$, $p < 0.01$) during readaptation
 507 (0.33 ± 0.06) (Fig. 5D), as well as the learning rate of the slow state (i.e. B_s) in adaptation ($0.024 \pm$
 508 0.01 , mean \pm SEM) was significantly increased (two-tailed t-test, $t(32) = 2.223$, $p < 0.05$) during
 509 readaptation (0.08 ± 0.03) (Fig. 5E).

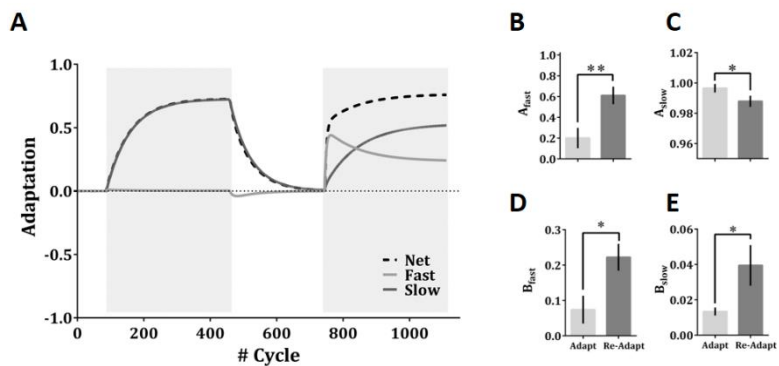
510 **Figure 5.** Adaptation of the slow and
 511 fast components of the varying
 512 parameters dual-rate SSM during
 513 experiment 2. **A.** The net (dashed
 514 black line), slow (dark gray line) and
 515 fast state (light gray line) estimates
 516 from the VP 2-Rate SSM to the
 517 across-subject averaged data. **B.**
 518 Forgetting rates of the fast process
 519 (i.e. A_{fast}) averaged across subjects



520 during adaptation (light gray bar) and readaptation (dark gray bar). **C.** Forgetting rates of the slow
 521 process (i.e. A_{slow}) averaged across subjects during adaptation (light gray bar) and readaptation (dark
 522 gray bar). **D.** Learning rates of the fast process (i.e. B_{fast}) averaged across subjects during adaptation
 523 (light gray bar) and readaptation (dark gray bar). **E.** Learning rates of the slow process (i.e. B_{slow})
 524 averaged across subjects during adaptation (light gray bar) and readaptation (dark gray bar). Error
 525 bars indicate SEM.

526 A similar picture is seen in experiment 3 (Fig. 6A), where both learning and forgetting rates of the
 527 slow and fast learning components have changed. The forgetting rate of the fast state (i.e. A_f) in
 528 adaptation (0.20 ± 0.1 , mean \pm SEM) was significantly lower (two-tailed t-test, $t(24)=3.182$
 529 $p<0.01$) than the forgetting rate of the fast state in readaptation (0.61 ± 0.08) (Fig. 6B), the
 530 forgetting rate of the slow state (i.e. A_s) in adaptation (0.996 ± 0.001) was also significantly higher
 531 (two-tailed t-test, $t(24)=2.305$ $p<0.05$) than the forgetting rate of the slow state in readaptation
 532 (0.987 ± 0.02) (Fig. 6C). Moreover, the learning rate of the fast state (i.e. B_f) in adaptation ($0.07 \pm$
 533 0.04) was significantly increased (two-tailed t-test, $t(24)=2.714$, $p<0.05$) during readaptation
 534 (0.22 ± 0.04) (Fig. 6D), and the learning rate of the slow state (i.e. B_s) in adaptation (0.013 ± 0.002 ,
 535 mean \pm SEM) was also significantly increased (two-tailed t-test, $t(24)=2.23$, $p<0.05$) during
 536 readaptation (0.04 ± 0.01) (Fig. 6E). From the fits of the averaged data presented in Fig 6A, it seems
 537 that the adaptation process could be captured by only a single slow state with no contribution of a
 538 fast state. Nevertheless, learning rates from the single-subject fits of the fast components of the
 539 adaptation phase tend to be higher than zero ($t(12)=2.1$, $p=0.06$ for A_f and $t(12)=1.9$, $p=0.08$ for
 540 B_f), suggesting that across subjects, the fast component did play a role in the initial adaptation
 541 block.

542 **Figure 6.** Adaptation of the slow and fast components of the varying
 543 parameters dual-rate SSM during
 544 varying parameters dual-rate SSM during
 545 experiment 3. **A.** The net (dashed
 546 black line), slow (dark gray line) and
 547 fast state (light gray line) estimates
 548 from the VP 2-Rate SSM to the
 549 across-subject averaged data. **B.**
 550 Forgetting rates of the fast process
 551 (i.e. A_{fast}) averaged across subjects
 552 during adaptation (light gray bar) and readaptation (dark gray bar). **C.** Forgetting rates of the slow
 553 process (i.e. A_{slow}) averaged across subjects during adaptation (light gray bar) and readaptation (dark
 554 gray bar). **D.** Learning rates of the fast process (i.e. B_{fast}) averaged across subjects during adaptation
 555 (light gray bar) and readaptation (dark gray bar). **E.** Learning rates of the slow process (i.e. B_{slow})
 556 averaged across subjects during adaptation (light gray bar) and readaptation (dark gray bar). Error
 557 bars indicate SEM.



558

559 Although initial bias did not reach significance levels, there was a trend towards a decrease in
560 initial error in readaptation compared to adaptation in both experiments (Fig 3D and 4D). In order
561 to obviate a possible bias influence on the estimation of learning parameters in our models during
562 the readaptation phase, we have added a free parameter in our varying parameters model that
563 represents an initial bias (e.g., a possible bias effect) during re-adaptation. Consistent with our
564 previous results, we found similar changes in learning parameters following initial learning.
565 Adding this additional parameter did not affect the AIC results favoring the VP models. Thus, our
566 suggested model is robust for possible bias effects.

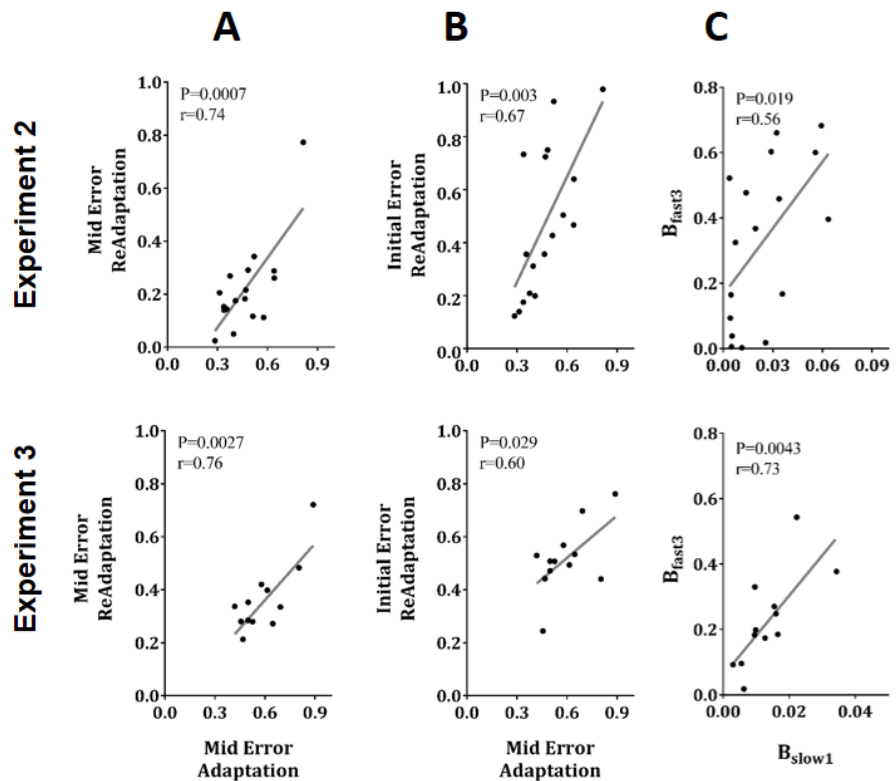
567

568 *Correlation of Savings, adaptation and learning parameters*

569 Previous attempts to explain savings used a linear time invariant model with two learning
570 components (LTI 2-Rate SSM), showing that the slow forgetting of the slow learning component
571 can account for various savings phenomena (Smith et al. 2006). Nevertheless, consistently with
572 the results of Zarahn et al. (2008), we show here that also in locomotor adaptation, models with
573 varying parameters account better for savings effects in adaptation-counterperturbation-
574 readaptation and adaptation-washout-readaptation paradigms, suggesting that different learning
575 parameters are expressed before and after learning. Still, the fact that learning parameters change
576 through learning does not mean that they are independent; it could be that the changes in
577 parameters following learning are correlated with their initial values. Such dependency will be
578 indicative of the mechanisms that give rise to savings. We therefore investigated the correlation of
579 error rates and learning parameters as seen in the inter-subject correlation patterns between
580 adaptation and readaptation blocks. We started by examining the inter-subject correlation of the
581 initial and middle error rates in the adaptation and readaptation phases. We found that both initial
582 errors and middle errors in readaptation significantly correlated with middle errors in the
583 adaptation phase (all comparisons reveal $0.60 \leq r \leq 0.76$ and $0.0007 \leq p \leq 0.029$, Fig. 7A and 7B),
584 indicating that early readaptation is correlated with on subjects' behavior during the initial
585 adaptation phase. We then moved to examining the correlation pattern of the estimated learning
586 parameters that could potentially provide a refined estimation of the source of correlation that we
587 have seen in error rates. We found that out of the 4 possible pairs of learning rate correlations (slow
588 and fast adaptation rates vs. slow and fast readaptation rates) in each experiment, only the slow
589 adaptation and fast readaptation learning parameters were significantly correlated in both
590 experiments [$r=0.56$, $P=0.019$ (Pearson correlation test) for experiment 2 (Fig. 7C, top panel) and
591 $r=0.73$, $P=0.0043$ for experiment 3 (Fig. 7C, bottom panel), respectively]. In both tests there are 4
592 comparisons which require correcting for false positive rates. Applying these corrections using
593 Bonferroni correction result in significant effect for the slow adaptation and fast readaptation
594 learning parameters for experiment 3 and a marginal result for experiment 2 ($p=0.019$ where the
595 corrected threshold was 0.0125). Nevertheless, the consistency of results in the two experiments,
596 and across the two measurements (of error rates and learning parameters) suggests that the
597 correlation between readaptation learning and the slow initial adaptation is not spurious.

598 Another concern about the current correlation results is that while the correlations between middle
 599 errors in adaptation and readaptation epochs were significant, the correlations of the slow learning
 600 parameters (i.e. Bs) in both these periods were not. At this point we cannot tell whether this
 601 apparent inconsistency is a due to the fact that the middle error correlations is driven by the
 602 correlation between the slow and fast learning parameters in the adaptation and readaptation
 603 epochs respectively, or due to our limited sensitivity to detect the correlations between the slow
 604 learning parameters in the two epochs.

605 **Figure 7.** Correlation of
 606 the errors and learning
 607 parameters during
 608 experiment 2 and 3. **A.**
 609 Cross-correlation
 610 between middle errors in
 611 adaptation and middle
 612 errors in readaptation
 613 during experiment 2 (top
 614 panel) and experiment 3
 615 (bottom panel). **B.** Cross-
 616 correlation between
 617 middle errors in
 618 adaptation and initial
 619 errors in readaptation
 620 during experiment 2 (top
 621 panel) and experiment 3
 622 (bottom panel). **C.** Cross-
 623 correlation between the
 624 slow adaptation
 625 parameter (i.e. B_{slow1}) and
 626 fast readaptation learning parameter (i.e. B_{fast3}) estimate from the VP 2-Rate SSM during experiment
 627 2 (top panel) and experiment 3 (bottom panel).



628

629 Discussion

630 Using the split-belt treadmill paradigm, we examined the learning mechanisms underlying
 631 adaptation and savings during the learning of a novel locomotor task. In the first experiment, we
 632 reanalyzed our previous results (Mawase et al. 2013) to establish the computational model of the
 633 basic learning process within a simple adaptation paradigm. However, the data from the first
 634 experiment missed an important phenomenon of motor learning: savings. Therefore, we designed
 635 two additional experiments to test for savings effects. Based on several experimental paradigms
 636 developed for reaching adaptation (Krakauer et al. 2005; Smith et al. 2006; Zarahn et al. 2008),

637 we chose the adaptation-counterperturbation-readaptation (i.e. experiment 2) and the adaptation-
638 washout-readaptation (i.e. experiment 3) protocols to test the underlying learning process for
639 savings. We found that while multiple-rate SSM can account for initial error reduction and
640 aftereffects of the simple adaptation paradigm (i.e. experiment 1), it failed to explain savings in
641 the second and the third experiments. Instead, we found that allowing the parameters of the dual-
642 rate state space learning process to change following initial learning can successfully explain
643 savings effects seen in both protocols. This supports the hypothesis that locomotor adaptation leads
644 to changes in the fast and slow learning parameters that would last beyond the decay of the hidden
645 state of the motor system. Furthermore, analyzing the inter-subject variability provides a
646 suggestive causal relationship between the slow and fast learning components before and after
647 learning, respectively. Particularly, we found that the fast relearning rate depends on the slow
648 learning rate during adaptation, suggesting that the magnitude of savings will be proportional to
649 the learning achieved during the prolonged exposure to adaptation. Together, these findings shed
650 new insights into the formation of motor memory.

651 Our model-comparison results are consistent with a recent study where savings effects in reaching
652 visuomotor adaptation paradigms were examined (Zarahn et al. 2008). Zarahn et al. (2008)
653 suggested a non-linear time invariant SSM to properly account for savings during the readaptation
654 phase. This non-linear behavior underlies the metalearning process by allowing changes in the
655 learning parameters in an experience-dependent manner. A key aspect of the model is that
656 consequent adaptation phases are associated with adjustable learning and forgetting rates. We
657 found significantly different learning and forgetting parameters across the phases of an adaptation
658 experiment (Fig.5 and Fig. 6). Suggestive changes in learning parameters can also be seen in a
659 recent locomotor adaptation study, where Malone et al. (2011) found that different adaptation
660 structures affect significantly the retention of the motor memory during readaptation on the
661 subsequent day. The faster relearning rate on the subsequent day provides evidence of the
662 involvement of a non-linear learning process in locomotor adaptation. While Malone's results were
663 not modeled, we show here that indeed a LTI model cannot account for several within-day savings
664 phenomena, and provide a suggestive underlying mechanism for this effect.

665 Recently, context-dependent linear models with either single or multiple slow states have been
666 suggested to explain savings during visuomotor rotation (Lee and Schweighofer 2009), force-field
667 adaptation (Pekny et al. 2011) and object rotation (Ingram et al. 2011). According to the context-
668 dependent learning approach, motor adaptation occurs through a fast and a slow contextual
669 learning process that are updated simultaneously by the same motor errors. Savings occur by
670 switching back to a previously learned internal model (slow process). A noticeable limitation of
671 the context-dependent model is that it does not account for consolidation after learning
672 (Criscimagna-Hemminger and Shadmehr 2008) or adaptation across days (Kording et al. 2007).
673 The fact that all the slow states decay with time needs to be refined, as subjects clearly retain across
674 days (Malone et al. 2011). Furthermore, the changes in the fast learning process following
675 adaptation suggest that savings cannot be explained only by the changes in slow learning

676 processes, and requires modification of the fast process as well, a property that does not exist in
677 the current context-dependent learning approach. Together, our behavioral and computational
678 results strongly lead to the conclusion that savings occurs through changes in learning parameters
679 (meta-learning) and not by switching between hidden learning states.

680 Although individuals learn differently a given motor task in terms of learning rates, most of the
681 previous studies focused on averaged learning rates measured across subjects, leaving the inter-
682 subject variability completely unexplored. In the current study, we studied the relationship
683 between the slow and fast learning components before and after learning. Using VP-2 SSM
684 parameters, we found a significant correlation between the slow learning rate during adaptation
685 and the fast learning rate during readaptation (Fig. 7). These results are also found when looking
686 at the correlation between initial and middle errors during adaptation and during readaptation
687 phases. Thus, the magnitude of savings for each subject was proportional to the learning achieved
688 by the slow learning process. These findings suggest that even though the varying parameters
689 model accounted for our result better than the fixed parameter model, learning parameters during
690 adaptation and readaptation are not independent, and may be subjected to a higher learning process
691 that modulates the learning parameters following learning. Our interpretation of the positive
692 correlation between the fast state during readaptation and the slow state during initial adaptation
693 is that savings is predominantly the outcome of a slow learning and slow decaying process of initial
694 adaptations. This conclusion is consistent with recent works that emphasize the role of the slow
695 process in long term retention (Joiner and Smith 2008), in estimation of the source of error
696 (Kording et al. 2007) and in savings in force field adaptation (Smith et al. 2006)

697 Despite multiple differences between reaching and locomotor adaptation, we found that learning
698 in both behaviors can be explained using the same VP models, and in both paradigms, savings
699 depend on the slow learning process. Thus, a reasonable conjecture is that the two learning
700 behaviors also share a similar neuronal basis. Two predominant brain areas are likely to be
701 involved in adaptation learning: cerebellum and motor cortex (Shmuelof and Krakauer 2011).
702 Several studies suggested that the cerebellum is involved in error based learning (Atkeson 1989;
703 Diedrichsen et al. 2005; Kawato et al. 1987; Miall et al. 2007;), and damage to the cerebellum
704 hampers the ability to adapt to external perturbations based on sensory prediction errors (Ilg et al.
705 2008; Maschke et al. 2004; Morton and Bastian 2006; 2004, Tseng et al. 2007). Recently, Jayaram
706 et al. (2012) used a non-invasive transcranial magnetic stimulation (TMS) to show that the
707 cerebellum excitability is modulated during locomotor adaptation. Furthermore, Galea et al. (2011)
708 found that non-invasive stimulation using tDCS over the cerebellum enhances error-reduction
709 during visuomotor reaching adaptation task. Interestingly, this stimulation did not affect
710 subsequent savings. Thus, the cerebellum is needed for adaptation learning in reaching and
711 locomotion, and is likely to affect the rate of the learning. The motor cortex, on the other hand, has
712 been shown to be involved in retention of adaptive patterns (savings), but not directly in adaptation,
713 as patients with stroke in the motor systems can adapt (Reisman et al. 2007; Scheidt et al. 2000;
714 Scheidt and Stoeckmann 2007). In the same study of Galea et al. (2011), stimulation over the

715 primary motor cortex did not change the learning rate of reaching adaptation, but increased its
716 subsequent savings (Galea et al. 2011). Taken together, while the cerebellum is likely to be vital
717 for the fast learning process, we speculate that the savings in our study depend on primary motor
718 cortex processes that are likely to affect behavior through the slow learning process. The fact that
719 we did find correlations between the slow learning process and the fast relearning process, suggests
720 that the two learning processes are not independent. It remained to be seen whether the
721 enhancement of the fast process is retained in the cerebellum or is the result of the feedforward
722 control over the locomotion pattern controlled by the cortex or by the controller itself, located in
723 the cortex and the spinal cord.

724 We conclude that adaptation and savings in locomotion occur through modulation of learning
725 parameters in a dual-rate model. These changes are consistent with results in reaching adaptation,
726 suggesting a common mechanism for savings, which is likely to depend on the motor cortex. It
727 would be interesting to investigate our within-day savings results with savings across days to
728 further elucidate the dynamics of parameter changes following initial adaptation.

729

730 **Acknowledgments**

731 This work was supported by the U.S Agency for International Development (USAID), The Middle
732 East Regional Cooperation Program (MERC), by Grant No. 74/12 from the Israel Science
733 Foundation (ISF), and by the Ministry of Science and Technology, Israel.

734

735 **References**

- 736 **Akaike H.** A new look at the statistical model identification. *Automatic Control, IEEE Transactions on* 19:
737 716-723, 1974.
- 738 **Atkeson CG.** Learning arm kinematics and dynamics. *Annual review of neuroscience* 12: 157-183, 1989.
- 739 **Benda BJ, Riley P, and Krebs D.** Biomechanical relationship between center of gravity and center of
740 pressure during standing. *Rehabilitation Engineering, IEEE Transactions on* 2: 3-10, 1994.
- 741 **Berniker M, and Kording KP.** Estimating the relevance of world disturbances to explain savings,
742 interference and long-term motor adaptation effects. *PLoS computational biology* 7: e1002210, 2011.
- 743 **Besser M, Kowalk D, and Vaughan C.** Mounting and calibration of stairs on piezoelectric force platforms.
744 *Gait & Posture* 1: 231-235, 1993.
- 745 **Criscimagna-Hemminger SE, and Shadmehr R.** Consolidation patterns of human motor memory. *The*
746 *Journal of Neuroscience* 28: 9610-9618, 2008.
- 747 **Diedrichsen J, Verstynen T, Lehman SL, and Ivry RB.** Cerebellar involvement in anticipating the
748 consequences of self-produced actions during bimanual movements. *Journal of neurophysiology* 93: 801,
749 2005.
- 750 **Donchin O, Francis JT, and Shadmehr R.** Quantifying generalization from trial-by-trial behavior of adaptive
751 systems that learn with basis functions: theory and experiments in human motor control. *Journal of*
752 *Neuroscience* 23: 9032, 2003.

753 **Galea JM, Vazquez A, Pasricha N, de Xivry J-JO, and Celnik P.** Dissociating the roles of the cerebellum and
754 motor cortex during adaptive learning: the motor cortex retains what the cerebellum learns. *Cerebral*
755 *Cortex* 21: 1761-1770, 2011.

756 **Heng C, and de Leon RD.** The rodent lumbar spinal cord learns to correct errors in hindlimb coordination
757 caused by viscous force perturbations during stepping. *The Journal of Neuroscience* 27: 8558-8562, 2007.

758 **Huang VS, Haith A, Mazzoni P, and Krakauer JW.** Rethinking motor learning and savings in adaptation
759 paradigms: model-free memory for successful actions combines with internal models. *Neuron* 70: 787-
760 801, 2011.

761 **Ilg W, Giese M, Gizewski E, Schoch B, and Timmann D.** The influence of focal cerebellar lesions on the
762 control and adaptation of gait. *Brain* 131: 2913-2927, 2008.

763 **Ingram JN, Howard IS, Flanagan JR, and Wolpert DM.** A single-rate context-dependent learning process
764 underlies rapid adaptation to familiar object dynamics. *PLoS computational biology* 7: e1002196, 2011.

765 **Jayaram G, Tang B, Pallegadda R, Vasudevan EV, Celnik P, and Bastian A.** Modulating locomotor
766 adaptation with cerebellar stimulation. *Journal of neurophysiology* 107: 2950-2957, 2012.

767 **Joiner WM, and Smith MA.** Long-term retention explained by a model of short-term learning in the
768 adaptive control of reaching. *Journal of neurophysiology* 100: 2948, 2008.

769 **Kawato M, Furukawa K, and Suzuki R.** A hierarchical neural-network model for control and learning of
770 voluntary movement. *Biological cybernetics* 57: 169-185, 1987.

771 **Kojima Y, Iwamoto Y, and Yoshida K.** Memory of learning facilitates saccadic adaptation in the monkey.
772 *The Journal of Neuroscience* 24: 7531-7539, 2004.

773 **Kording KP, Tenenbaum JB, and Shadmehr R.** The dynamics of memory as a consequence of optimal
774 adaptation to a changing body. *Nature Neuroscience* 10: 779-786, 2007.

775 **Krakauer JW, Ghez C, and Ghilardi MF.** Adaptation to visuomotor transformations: consolidation,
776 interference, and forgetting. *The Journal of Neuroscience* 25: 473-478, 2005.

777 **Lee JY, and Schweighofer N.** Dual adaptation supports a parallel architecture of motor memory. *The*
778 *Journal of Neuroscience* 29: 10396-10404, 2009.

779 **Malone LA, Vasudevan EVL, and Bastian AJ.** Motor Adaptation Training for Faster Relearning. *The Journal*
780 *of Neuroscience* 31: 15136-15143, 2011.

781 **Maschke M, Gomez CM, Ebner TJ, and Konczak J.** Hereditary cerebellar ataxia progressively impairs force
782 adaptation during goal-directed arm movements. *Journal of neurophysiology* 91: 230-238, 2004.

783 **Mawase F, Haizler T, Bar-Haim S, and Karniel A.** Kinetic adaptation during locomotion on a split-belt
784 treadmill. *Journal of neurophysiology* 109: 2216-2227, 2013.

785 **Miall RC, Christensen LO, Cain O, and Stanley J.** Disruption of state estimation in the human lateral
786 cerebellum. *PLoS biology* 5: e316, 2007.

787 **Morton SM, and Bastian AJ.** Cerebellar contributions to locomotor adaptations during splitbelt treadmill
788 walking. *The Journal of Neuroscience* 26: 9107-9116, 2006.

789 **Morton SM, and Bastian AJ.** Cerebellar control of balance and locomotion. *The Neuroscientist* 10: 247-
790 259, 2004.

791 **Pekny SE, Criscimagna-Hemminger SE, and Shadmehr R.** Protection and expression of human motor
792 memories. *The Journal of Neuroscience* 31: 13829-13839, 2011.

793 **Reisman DS, Block HJ, and Bastian AJ.** Interlimb coordination during locomotion: what can be adapted
794 and stored? *Journal of neurophysiology* 94: 2403-2415, 2005.

795 **Reisman DS, Wityk R, Silver K, and Bastian AJ.** Locomotor adaptation on a split-belt treadmill can improve
796 walking symmetry post-stroke. *Brain* 130: 1861-1872, 2007.

797 **Robinson FR, Soetedjo R, and Noto C.** Distinct short-term and long-term adaptation to reduce saccade
798 size in monkey. *Journal of neurophysiology* 96: 1030-1041, 2006.

799 **Roerdink M, Coolen B, Clairbois B, Lamoth CJC, and Beek PJ.** Online gait event detection using a large
800 force platform embedded in a treadmill. *Journal of Biomechanics* 41: 2628-2632, 2008.

801 **Scheidt RA, Reinkensmeyer DJ, Conditt MA, Rymer WZ, and Mussa-Ivaldi FA.** Persistence of motor
802 adaptation during constrained, multi-joint, arm movements. *Journal of neurophysiology* 84: 853, 2000.
803 **Scheidt RA, and Stoeckmann T.** Reach adaptation and final position control amid environmental
804 uncertainty after stroke. *Journal of neurophysiology* 97: 2824-2836, 2007.
805 **Shadmehr R, and Brashers-Krug T.** Functional stages in the formation of human long-term motor memory.
806 *The Journal of Neuroscience* 17: 409-419, 1997.
807 **Shadmehr R, and Mussa-Ivaldi FA.** Adaptive representation of dynamics during learning of a motor task.
808 *The Journal of Neuroscience* 14: 3208-3224, 1994.
809 **Shmuelof L, and Krakauer JW.** Are we ready for a natural history of motor learning? *Neuron* 72: 469-476,
810 2011.
811 **Smith MA, Ghazizadeh A, and Shadmehr R.** Interacting adaptive processes with different timescales
812 underlie short-term motor learning. *PLoS Biol* 4: e179, 2006.
813 **Thoroughman KA, and Shadmehr R.** Learning of action through adaptive combination of motor primitives.
814 *Nature* 407: 742-747, 2000.
815 **Tseng Y, Diedrichsen J, Krakauer JW, Shadmehr R, and Bastian AJ.** Sensory prediction errors drive
816 cerebellum-dependent adaptation of reaching. *Journal of neurophysiology* 98: 54-62, 2007.
817 **Zarahn E, Weston GD, Liang J, Mazzoni P, and Krakauer JW.** Explaining savings for visuomotor adaptation:
818 linear time-invariant state-space models are not sufficient. *Journal of neurophysiology* 100: 2537-2548,
819 2008.

820

821

822 **Tables**

823 **Table 1.** Across-subject averages of the SSM parameters during phase 1 (i.e. adaptation) and
 824 phase 3 (i.e. readaptation) of experiment 2 and 3. VP Dual-Rate represents the varying
 825 parameters dual-rate SSM and VP Single-Rate represents the varying parameters single-rate
 826 SSM. Values are mean with SEMs in parentheses. N/A parameter not applicable for that
 827 model.

828

	VP Dual-Rate	VP Single-Rate	LTI Dual-rate
<i>Experiment 2</i>			
<i>Phase 1</i>			
A_{fast}	0.4254±(0.1061)	N/A	0.4403±(0.099)
A_{slow}	0.9962±(0.001)	0.9952±(0.001)	0.9986±(0.001)
B_{fast}	0.1006±(0.035)	N/A	0.0861±(0.036)
B_{slow}	0.0241±(0.005)	0.0227±(0.005)	0.0092±(0.002)
D	1.2740±(0.047)	1.0511±(0.062)	0.8191±(0.045)
<i>Phase 3</i>			
A_{fast}	0.7147±(0.0590)	N/A	N/A
A_{slow}	0.9724±(0.0155)	0.9445±(0.019)	N/A
B_{fast}	0.3283±(0.0596)	N/A	N/A
B_{slow}	0.0837±(0.0263)	0.3120±(0.065)	N/A
D	1.2740±(0.047)	1.0511±(0.062)	N/A

<i>Experiment 3</i>			
<i>Phase 1</i>			
A_{fast}	0.2011±(0.0976)	N/A	0.4778±(0.1245)
A_{slow}	0.9965±(0.0008)	0.9959±(0.0008)	0.9949±(0.0016)
B_{fast}	0.0739±(0.0394)	N/A	0.0646±(0.0242)
B_{slow}	0.0134±(0.0023)	0.0134±(0.0024)	0.0139±(0.0032)
D	1.3078±(0.0688)	1.1871±(0.0676)	1.2086±(0.0597)
<i>Phase 3</i>			
A_{fast}	0.6103±(0.0837)	N/A	N/A
A_{slow}	0.9879±(0.0037)	0.9767±(0.0052)	N/A
B_{fast}	0.2222±(0.0379)	N/A	N/A
B_{slow}	0.0395±(0.0115)	0.0756±(0.0171)	N/A
D	1.3078±(0.0688)	1.1871±(0.0676)	N/A
